JOURNAL OF APPLIED ELECTROCHEMISTRY 17 (1987) 329–339

Selectivity characteristics of the electrohydrodimerization of acrylonitrile

K. SCOTT, I. F. McCONVEY, J. HENDERSON

Department of Chemical Engineering, Teesside Polytechnic, Middlesbrough, Cleveland, TS1 3BA, UK

Received 11 March 1986

A mathematical model of a reaction scheme for the electrohydrodymerization of acrylonitrile to adiponitrile in a loop reactor is presented. This model, which is based on a plug flow reactor with a recycle loop and continuous removal of product, is used to simulate steady-state operation at various operating conditions. The effect of flowrate, current density and mass transport are investigated in terms of their effect on product distributions and selectivity. Overall, the reaction model deals with the formation of five products from the cathodic reactions.

Nomenclature

C_j	bulk concentration of species j ($mol\,m^{-3}$)
C_j^s	surface concentration of species j ($mol\,m^{-3}$)
C_{jo}	initial concentration of species j ($mol\,m^{-3}$)
C_{jp}	cell exit concentration of species j ($mol\,m^{-3}$)
F	Faraday constant
i_k	current density of reaction step k ($A\,m^{-2}$)
i_T	total applied current density ($A\,m^{-2}$)
i_{AN}	current density for acrylonitrile reduction ($A\,m^{-2}$)
k_L	mass transfer coefficient ($m\,s^{-1}$)
k_i	rate constant of step i
n_k	number of electrons transferred in step k
N_j	number of mols of species j (mol)
S	selectivity
Q	electrolyte flow rate ($m^3\,s^{-1}$)
V	cell volume (m^3)
X_A	conversion
Y_D	yield of adiponitrile
τ	residence time (s)
σ	electrode area (m^2)
Re	Reynolds number based on hydraulic mean diameter

Subscripts

A	acrylonitrile
P	propionitrile
T	trimer
BCN	biscyanoethylether
HOPN	hydroxypropionitrile
O	cell inlet condition
P	cell outlet condition

1. Introduction

In chemical engineering, process modelling and simulation is of prime importance in gaining an understanding of a process. One objective of modelling and simulation is to explore the effects of different operating conditions on system performance. This may be to evaluate control strategies, carry out optimization studies or for troubleshooting purposes. A major incentive for this is that simulations are usually much cheaper, faster and safer than experimental tests on operating units. From simulations the effect of changes in process operating parameters on product distributions can be determined.

0021-891X/87 $03.00 + .12 © 1987 Chapman and Hall Ltd.

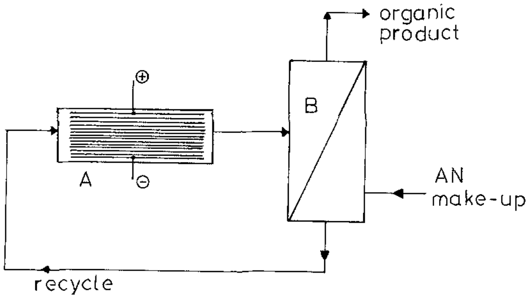

Fig. 1. Schematic diagram of recycle reactor unit.

This communication describes a brief application of this area of chemical engineering to an electrochemical process, the production of adiponitrile. The behaviour of the reactor unit (in the form of a bank of cells plus a phase separator) in terms of its response to changes in mass transport rates and recycle rates is considered. The study is based around a previously described reaction mechanism for the electrohydrodimerization of acrylonitrile [1] which has been extended to include the effect of mass transport on reaction rates and the formation of by-products from cyanoethylation reactions of acrylonitrile.

2. Reactor model for electrohydrodimerization of acrylonitrile to adiponitrile

2.1. *Reactor system*

A simplified schematic diagram of the recycle reactor unit is shown in Fig. 1. The cell banks A (parallel plate electrodes with approximately plug flow characteristics) are continuously supplied with aqueous electrolyte containing acrylonitrile, recycled from the separator (B). In the reactor a second organic product phase is formed (from the cathodic reduction of acrylonitrile), which on passing to the phase separator is decanted off the aqueous phase. The organic phase (upper layer) is then processed in the separation trains to produce a crude adiponitrile product and a recycle acrylonitrile stream which is eventually returned to the phase separator as make-up.

2.2. *Reaction model*

The mechanism for the electrohydrodimerization of acrylonitrile is based on a previous analysis of batch electrolysis data [1]. Under the conditions of the work three main products result from this reaction: adiponitrile (D), propionitrile (P) and 1,3,6-tricyanohexane (T), known as trimer. The reaction mechanism can be represented as follows:

$$\begin{tikzcd}
A \arrow[r, "1"'] & B \arrow[r, "+A+H^+", "3"'] \arrow[d, "2"', "+2H^+"] & C \arrow[r, "+H^+", "5"'] \arrow[d, "4"', "+A \; +H^+"] & D \\
& P & T &
\end{tikzcd} \qquad (1)$$

In this mechanism B may be the radical anion and C an anion intermediate.

An alternative reaction mechanism has been proposed by Arad *et al.* [2] which satisfies the chemistry associated with adiponitrile production, in which acrylonitrile undergoes electrochemical reduction to a dianion intermediate prior to a sequence of chemical reactions. The intermediate B either reacts further with acrylonitrile A to form an adiponitrile dianion intermediate C or undergoes an overall reaction with water to propionitrile. The intermediate C then either reacts with acrylonitrile to form the trimeric product (T) or is converted to adiponitrile. The mechanism proposed by Arad *et al.* [2], together with the formation of trimer, is similar to that scheme proposed above. In this case electron exchange is associated with only the first step, i.e. the reduction of acrylonitrile to a dianion, the intermediate B.

Steady-state reactor material balances for the proposed mechanism are written as follows:

$$\frac{-\mathrm{d}N_A}{\mathrm{d}\tau} = \sigma C_A^s(k_1 + k_3 C_B^s + k_4 C_C^s) \tag{2}$$

$$\frac{\mathrm{d}N_B}{\mathrm{d}\tau} = \sigma(k_1 C_A^s - k_2 C_B^s - k_3 C_A^s C_B^s) \tag{3}$$

$$\frac{\mathrm{d}N_P}{\mathrm{d}\tau} = \sigma k_2 C_B^s \tag{4}$$

$$\frac{\mathrm{d}N_C}{\mathrm{d}\tau} = \sigma(k_3 C_A^s C_B^s - k_4 C_A^s C_C^s - k_5 C_C^s) \tag{5}$$

$$\frac{\mathrm{d}N_D}{\mathrm{d}\tau} = \sigma k_5 C_C^s \tag{6}$$

$$\frac{\mathrm{d}N_T}{\mathrm{d}\tau} = \sigma k_4 C_A^s C_C^s \tag{7}$$

In the case of electrochemical reaction, the rate constant is of the Tafel type defined through the following equation:

$$\frac{i_1}{n_1 F} = k_1 C_A^s = k_f \exp(\beta_E) C_A^s \tag{8}$$

where k_f and β are the characteristic constants of the Tafel equation.

In the reaction system the intermediates B and C are not formed in significant amounts and hence the stationary state approximation is applied to Equations 3 and 5, i.e.

$$C_B^s = \frac{k_1 C_A^s}{k_2 + k_3 C_A^s} \tag{9}$$

$$C_C^s = \frac{\mathrm{k}_3 C_A^s C_B^s}{k_5 + \mathrm{k}_4 C_A^s} \tag{10}$$

The current density of step 1 of the reaction scheme can be written in terms of mass transport

$$\frac{i_1}{n_1 F} = k_L(C_A - C_A^s) \tag{11}$$

hence the surface and bulk concentrations of A are related according to the following equation:

$$C_A = \left(1 + \frac{k_1}{k_L}\right) C_A^s \tag{12}$$

3. Reactor model solution

Although industrial operation of the adiponitrile electrochemical reactor is at constant current, the simpler case (mathematically) of potentiostatic operation is considered first to act as an indicator to reactor behaviour, bearing in mind that if the reactor is operated with a low conversion per pass, there are only small changes in electrode potential over the electrode length.

3.1. *Potentiostatic operation*

The solutions of Equations 2 to 7 for potentiostatic operation is achieved in a space time-independent mode by dividing both Equations 4 and 7 by Equation 2, incorporating Equations 9, 10 and 12 and integrating to give:

$$\frac{\Delta N_T}{V\left(1+\dfrac{k_1}{k_L}\right)} = \left[\frac{C_A^s}{3} - \frac{b}{18}\ln(X) + \left(\frac{b^2-6a}{18U}\right)\ln\left(\frac{6C_A^s+b-U}{6C_A^s+b+U}\right)\right]_{C_{Ap}^s}^{C_{AO}^s} = \Psi_1(A) \quad (13)$$

$$\frac{\Delta N_P}{V\left(1+\dfrac{k_1}{k_L}\right)} = \frac{k_2}{k_3}\left[\left(\frac{k_5}{k_4}-\frac{b}{6}\right)\frac{1}{U}\ln\left(\frac{6C_A^s+b-U}{6C_A^s+b+U}\right) + \tfrac{1}{6}\ln(X)\right]_{C_{Ap}^s}^{C_{AO}^s} = \Psi_2(A) \quad (14)$$

where

$$b = \frac{k_2}{k_3} + \frac{2k_5}{k_4}$$

$$a = \frac{k_5 k_2}{k_4 k_3}$$

$$X = 3(C_A^s)^2 + bC_A^s + a$$

$$U = (b^2 - 12a)^{\frac{1}{2}} \quad (b^2 > 12a)$$

ΔN_T and ΔN_P are the moles trimer and propionitrile formed in the organic phase, respectively. An overall material balance gives the number of moles of adiponitrile.

In practice, on formation of the product organic phase, there is a redistribution of components, especially acrylonitrile, between phases. However, due to the relatively small reactor residence time, the redistribution of organic products between the aqueous electrolyte and the organic phase occurs primarily in the separator where acrylonitrile make-up is added. A typical organic phase from the separator contains 55–60% adiponitrile and 25–30% acrylonitrile.

In Equations 13 and 14 the inlet and outlet surface concentrations of the reactor are related to the respective bulk concentrations according to Equation 12.

From Equations 13 and 14 it is clear that system performance is governed by two ratios of rate constants, k_5/k_4 and k_2/k_3. Typical variations in product selectivities ($S_1 = \Delta N_D/\Delta N_P$, $S_2 = \Delta N_D/\Delta N_T$) with fractional conversion determined using kinetic data from [1] are shown in Fig. 2 for an initial concentration of acrylonitrile of 750 mol m^{-3}. Large variations in both selectivities are seen: S_1 decreasing with conversion as the reaction to adiponitrile is more dependent on the surface concentration of acrylonitrile than is the reaction to propionitrile and, conversely, S_2 increases with conversion. The yields of adiponitrile vary little (89–93%) over the range of conditions considered. In the electrolytic production of adiponitrile the reaction selectivities have particular bearing on product recovery and the separation trains downstream. Of particular relevance is the saleability of propionitrile. Clearly, conditions of reactor operation cannot be achieved where both byproducts are minimized and a compromise in selectivities is inevitable during operation.

Variations in values of selectivity shown in Fig. 2 are clearly dependent on the mass transfer characteristics pertaining to cell operation. A high mass transport rate favours the selectivity, S_1, i.e. gives relatively low amounts of propionitrile while resulting in greater yields of trimer. This is considered in more detail in the following section.

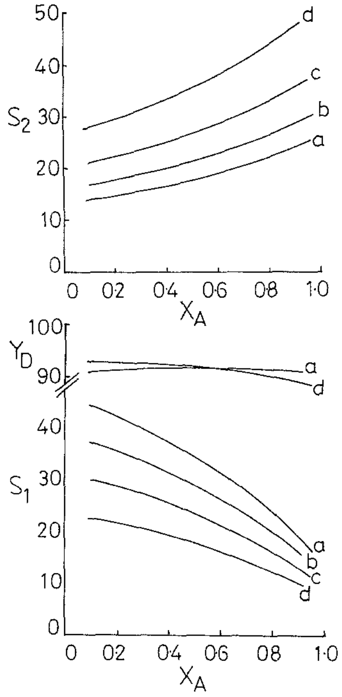

Fig. 2. Variation of selectivities with conversion in the reduction of acrylonitrile to adiponitrile. $S_1 = \Delta N_D/\Delta N_P$; $S_2 = \Delta N_D/\Delta N_T$; $Y_D = \Delta N_D/\Delta N_A$. Values of k_2/k_3 and k_5/k_4 are 30 and 1.5×10^{-4}, respectively, for curves a–d. Values of k_1/k_L are: (a) 0; (b) 0.2; (c) 0.5; (d) 1.

3.2. *Galvanostatic operation*

The analysis of the adiponitrile reactor during constant current operation incorporates the reaction mechanism of Arad *et al.* [2]. It is felt that this mechanism adequately represents industrial behaviour and thus is sufficient to meet one of the aims of process modelling, i.e. the investigation of dynamic behaviour and process control strategies. This, however, is beyond the scope of this communication but is the subject of further work. For galvanostatic operation of the recycle reactor unit it is assumed that, with the relatively low conversions experienced in practice, the current is uniformly distributed over the electrodes.

With the assumption that the production of the by-product hydrogen is small (in practice approximately 5–10% of the total current consumed) and that its current density is proportional to the total current density of operation (i_T), i.e.

$$i_H = \alpha i_T \tag{15}$$

the reactor design equations can be solved (without numerical procedures previously described [3]) in a similar manner used in Section 3.1.

Consider first the solution for the change of acrylonitrile concentration in the aqueous phase with residence time. The bulk concentration of acrylonitrile from Equation 11 is a linear function of its surface concentration according to

$$C_A = C_A^s + \frac{i_{AN}}{n_1 F k_L} \tag{16}$$

where i_{AN} is the current density associated with the production of organic species and is written as

$$i_{AN} = i_T(1 - \alpha) = n_1 F k_1 C_A^s \tag{17}$$

It is assumed that the reaction step 1 operates exclusively at sub-limiting current conditions.

By combining Equation 2 with Equations 9, 10 and 17 the material balance for acrylonitrile can be written as

$$\frac{i_{\mathrm{T}}(1-\alpha)\sigma}{n_1 FV} = -\left[\frac{\left(\frac{k_2}{k_3}+C_{\mathrm{A}}^{\mathrm{s}}\right)\left(\frac{k_5}{k_4}+C_{\mathrm{A}}^{\mathrm{s}}\right)}{3(C_{\mathrm{A}}^{\mathrm{s}})^2+bC_{\mathrm{A}}^{\mathrm{s}}+a}\right]\left(\frac{\mathrm{d}C_{\mathrm{A}}}{\mathrm{d}\tau}\right) \tag{18}$$

On integration this equation gives

$$\frac{i_{\mathrm{T}}(1-\alpha)\sigma\tau}{n_1 FV} = \left[\frac{C_{\mathrm{A}}^{\mathrm{s}}}{3}+\left(\frac{\varepsilon}{6}-\frac{b}{18}\right)\ln(X)+\left(\frac{b^2-6a}{18}+a-\frac{b\varepsilon}{6}\right)\frac{1}{U}\ln\left\{\frac{(6C_{\mathrm{A}}^{\mathrm{s}}+b-U)}{(6C_{\mathrm{A}}^{\mathrm{s}}+b+U)}\right\}\right]_{C_{\mathrm{A_p}}^{\mathrm{s}}}^{C_{\mathrm{A_o}}^{\mathrm{s}}} \tag{19}$$

where $\varepsilon = (k_2/k_3) + (k_5/k_4)$.

The solutions to the material balances for propionitrile and trimer are obtained in a space time-independent mode as

$$\frac{\Delta N_{\mathrm{T}}}{V} = \Psi_1(A) \tag{20}$$

$$\frac{\Delta N_{\mathrm{P}}}{V} = \Psi_2(A) \tag{21}$$

At this point it is worth drawing attention to the effect of mass transport on behaviour and its role in Equations 19 to 21. Equation 19 relates the change between the inlet and outlet concentrations at the cathode surface to a number of reactor parameters, e.g. $i_{\mathrm{T}}(1-\alpha)$. These surface concentrations constitute the boundaries of the reactor whose bulk concentrations are related to surface concentrations through Equation 16 and hence depend significantly on the mass transfer coefficient. This therefore has an ongoing effect on the bulk production of organic products (Equations 20 and 21). The reactor is therefore modelled as a pseudo steady-state, heterogeneous reactor with fully developed concentration profiles.

3.3. *Reactor simulations*

This section considers the performance of the adiponitrile reactor during galvanostatic operation. The present industrial synthesis of adiponitrile uses undivided cells with an interelectrode gap of approximately 2 mm [4] and is probably the cheapest of the many types of electrolytic reactors available. This small cell gap gives low electrolyte ohmic losses while presumably still being large enough to prevent electrode shorting caused by solid material formed from the downstream processing and electrode corrosion. Little can probably be gained by adjusting this cell gap.

Fig. 3 shows the product distributions of adiponitrile, propionitrile and trimer as functions of current density and inlet acrylonitrile concentration for a typical electrolyte velocity of 1 m s^{-1} [4]. The trends in the product distribution are comparable to the experimental data of Childs and Walters [5], where the yield of trimer decreases and that of propionitrile increases with current density. In this case, with the low cell residence times used, the conversions are only approximately 5%, whereas Childs and Walters data is for a 50% conversion.

The effect of decreasing the inlet concentration of acrylonitrile is to decrease the amount of trimer while increasing propionitrile formation and eventually resulting in a drop in adiponitrile yield. This behaviour is expected in a reaction mechanism where products result from the surface chemical reaction between a reactant A and an intermediate formed from the reactant.

As was seen in Section 3.1, the mass transfer rate or coefficient is a major parameter affecting performance. High mass transfer rates are essential to ensure operation at high economic current

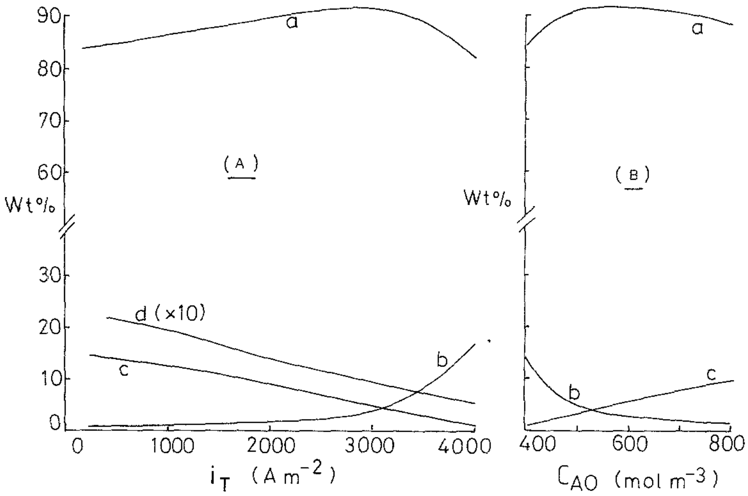

Fig. 3. Product distributions in adiponitrile synthesis. $Q = 3 \times 10^{-3}\,\mathrm{m\,s^{-1}}$; $\sigma = 3\,\mathrm{m}^2$, cell gap = $2 \times 10^{-3}\,\mathrm{m}$; $k_2/k_3 = 15.5\,\mathrm{mol\,m^{-3}}$; $k_5/k_4 = 6000\,\mathrm{mol\,m^{-3}}$. (A) The effect of current density, $C_{A_0} = 750\,\mathrm{mol\,m^{-3}}$ a, Adiponitrile; b, propionitrile; c, trimer; d, BCN. (B) The effect of inlet concentration. $i_T = 2000\,\mathrm{A\,m^{-2}}$. a, Adiponitrile; b, propionitrile; c, trimer; d, BCN.

densities (above limiting current conditions) with the low acrylonitrile concentrations used in practice. Electrolyte flow is turbulent and is supplied by the recycle stream from the decanter. This flow, which dictates the mass transport rates in the cells and the residence times, constitutes a major power cost to the process and hence any reductions in its operating value will be advantageous, providing reaction selectivity is maintained.

The effect of variations in recycle flow rate on reactor performance is shown in Fig. 4. The general behaviour is similar to that of the effect of acrylonitrile concentration in Fig. 3b. In this simulated behaviour a typical mass transfer correlation [6] of the Dittus Boelter type for parallel plate cells is adopted,

$$k_L = \bar{k}Re^{0.8} \tag{22}$$

where Re is the Reynolds number based on the hydraulic mean diameter of the channel. In the absence of suitable mass transfer correlations pertaining to cell operation, i.e. simultaneous oxygen and hydrogen evolution in a narrow channel, the above correlation is felt to be adequate for purpose of the simulation.

The results of Fig. 4 indicate that operation at velocities significantly less than $1\,\mathrm{m\,s^{-1}}$ (the quoted industrial value [4]) is feasible, although as the limiting current for acrylonitrile reduction is

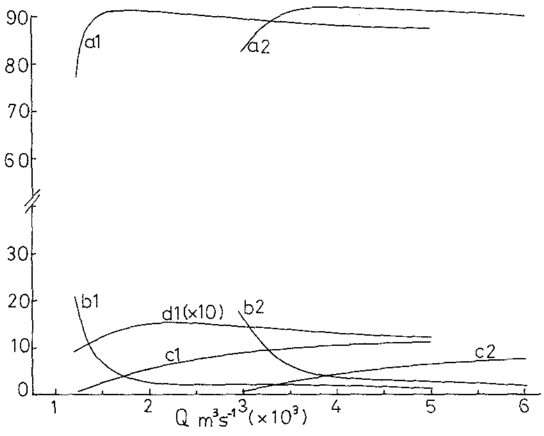

Fig. 4. Effect of flow rate on product distribution; parameters as Fig. 3. 1, $2000\,\mathrm{A\,m^{-2}}$; 2, $4000\,\mathrm{A\,m^{-2}}$.

approached a rapid fall-off in adiponitrile yield is seen. It is also shown that for operation at higher current densities, i.e. 4000 A m^{-2}, cell flow rates need to be significantly higher to maintain good yields of adiponitrile.

4. The influence of cyanoethylation reactions

Cyanoethylation reactions occurring during the synthesis of adiponitrile are [4]

$$\begin{array}{lcl} \underset{\text{acrylonitrile (A)}}{CH_2{=}CHCN} + H_2O & \xrightarrow{OH^-} & \underset{\text{hydroxypropionitrile (HOPN)}}{HOCH_2CH_2CN} \\ CH_2{=}CHCN + HOCH_2CH_2CN & \xrightarrow{OH^-} & \underset{\text{biscyanoethylether (BCN)}}{CN(CH_2)_2O(CH_2)_2CN} \end{array} \tag{23}$$

These two by-products, HOPN and BCN, are favoured under conditions of poor mass transport when a region of high pH at the electrode surface results from the electrolytic reactions. BCN appears to be the major by-product of the two reported [4]; HOPN is formed primarily from the thermal decomposition of BCN in the reboiler of the distillation column which also regenerates acrylonitrile. To introduce these reactions into the adiponitrile reactor simulation requires a knowledge of their respective rate constants.

4.1. *Estimation of cyanoethylation reaction rate constants*

Data for the production of cyanoethylation by-products during the continuous electrosynthesis of adiponitrile in a parallel plate flow cell is available [4] (see Fig. 6) in the form of percentage of by-product versus both linear velocity and Reynolds number. The conditions of operations are essentially those of the Monsanto divided cell process, using cell gaps of 0.8 to 2.4 mm, a constant temperature and a constant initial acrylonitrile concentration (16 wt %, i.e. 3000 mol m^{-3}).

Assuming that Reactions 23 are irreversible and first order with respect to the reactive constituents and OH$^-$, the reaction rate equations can be written as

$$\frac{dN_{HOPN}}{d\tau} = \sigma(k_9 C^s_A C^s_{OH^-} - k_{10} C^s_A C^s_{OH^-} C^s_{HOPN}) \tag{24}$$

$$\frac{dN_{BCN}}{d\tau} = \sigma k_{10} C^s_A C^s_{OH^-} C^s_{HOPN} \tag{25}$$

To simplify the analysis of these equations, as BCN is the major reported by-product, the stationary state approximation is applied to HOPN production (i.e. $dN_{HOPN}/d\tau = 0$) giving

$$\frac{dN_{BCN}}{d\tau} = \sigma k_9 C^s_A C^s_{OH^-} \tag{26}$$

Both the concentration of hydroxide ion and acrylonitrile ion at the electrode surface can be expressed in terms of mass transport equations

$$C^s_{OH^-} = C_{OH^-} + \frac{i_T}{Fk_L} \tag{27}$$

$$C^s_A = C_A - \frac{i_T - i_H}{2Fk_L} \tag{28}$$

assuming that the mass transfer coefficients of both species are identical. The bulk electrolyte pH during electrolysis is between 7 and 8 and hence C_{OH^-} is assumed to be negligible. Substituting

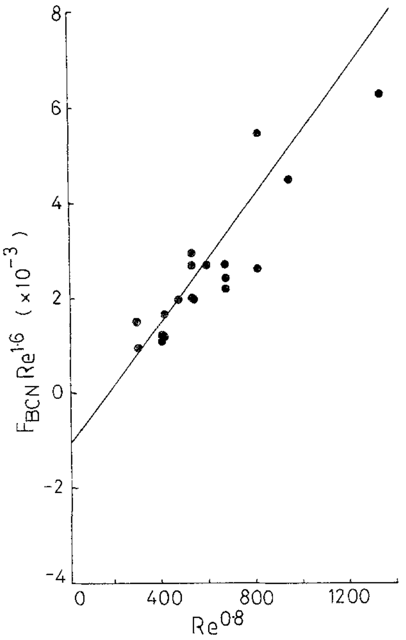

Fig. 5. Correlation of cyanoethylation by-products with Reynolds number.

Equations 27 and 28 into Equation 26 gives

$$\frac{dN_{BCN}}{d\tau} = \frac{\sigma k_9 i_T}{Fk_L}\left(C_A - \frac{i_T - i_H}{2Fk_L}\right) \tag{29}$$

When the conversion per pass in the flow cell is small the bulk concentration of acrylonitrile remains effectively constant, which allows a straightforward integration of Equation 29 to give

$$N_{BCN} = \frac{\sigma k_9 \tau i_T}{Fk_L}\left(C_A - \frac{i_T - i_H}{2Fk_L}\right) \tag{30}$$

for a constant current density. This equation, describing the moles of BCN produced as a function of cell parameters and in particular the mass transfer coefficient, is used after some re-arrangement to obtain the rate constant k_9.

4.1.1. Data analysis. As a good approximation the total moles of organic products is given by $(i_T \sigma \tau)/2F$, and hence the fraction of BCN in the product is given by:

$$F_{BCN} = \frac{2FN_{BCN}}{i_T \sigma \tau} = \frac{2k_9}{k_L}\left(C_A - \frac{i_T - i_H}{2Fk_L}\right) \tag{31}$$

Using a mass transfer correlation in the form of Equation 22, Equation 31 can be rearranged to give

$$F_{BCN} Re^{1.6} = \frac{2k_9 C_A}{\bar{k}} Re^{0.8} - \frac{k_9(i_T - i_H)}{F\bar{k}^2} \tag{32}$$

This equation gives a reasonable correlation (Fig. 5) of experimental data from [4] with the following slope and intercept:

$$\text{Slope} = \frac{2k_9 C_A}{\bar{k}} = 67$$

$$\text{Intercept} = \frac{k_9(i_T - i_H)}{F\bar{k}^2} = -1.16 \times 10^4$$

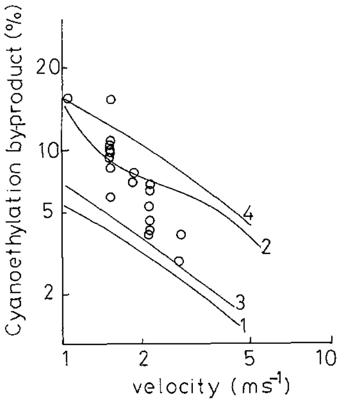

Fig. 6. Predicted variation of cyanoethylation by-products with linear electrolyte velocity. Current density ($\mathrm{A\,m^{-2}}$): (1, 2) 4500; (3, 4) 2000. Cell gap (mm): (1, 3) 2.5, (2, 4) 0.8. ○, Experimental data from [4].

To calculate k_9 from either the slope or intercept requires a value for $\bar{k}$. Experimental mass transfer data for parallel plate flow cells [6] gives a value of $\bar{k} = 3.8 \times 10^{-8}\,\mathrm{m\,s^{-1}}$ and hence from the slope, $k_9 = 4.24 \times 10^{-10}\,\mathrm{m\,s^{-1}\,(mol\,m^{-3})^{-1}}$. Alternatively, by dividing the square of the slope by the intercept, the value of k_9 can be estimated without reference to $\bar{k}$, if a value of $(i_T - i_H)$ is known. Assuming that $i_T = 4500\,\mathrm{A\,m^{-2}}$ (the quoted optimum [4]) and that the current efficiency for hydrogen formation is 5%, then $k_9 = 4.6 \times 10^{-10}\,\mathrm{m\,s^{-1}\,(mol\,m^{-3})^{-1}}$, which is in good agreement with the previous value.

In the above analysis it is assumed that the reaction of HOPN is fast and that the major by-product from Reaction 23 is BCN. In fact both species are formed and hence the rate constant k_9 should be considered to be applicable to the sum of the HOPN and BCN formation. Future reference to BCN implies the sum of both these species.

4.2. *Production of cyanoethylation by-products*

Using a mean value of $k_9 = 4.42 \times 10^{-10}\,\mathrm{m\,s^{-1}\,(mol\,m^{-3})^{-1}}$ it is shown in Fig. 6 that Equation 31 gives predicted values of the percentage of by-product that are in reasonable agreement with experimental data. The predicted behaviour for cell gaps of 0.8 and 2.4 mm and total current densities of 2000 and $4500\,\mathrm{A\,m^{-2}}$ virtually encompass the experimental points. Hence within the range of velocities used, Equation 30 can predict cyanoethylation by-product formation with reasonable confidence. However, it should be applied with caution at low velocities where it predicts a maximum in the by-product formation; something not reported and contrary to some experimental data. Here a more rigorous treatment is required, which includes the formation of BCN along with that of propionitrile, trimer and adiponitrile.

The reactor material balance for A and BCN are, in this case

$$-\frac{\mathrm{d}N_A}{\mathrm{d}\tau} = \sigma C_A^s(k_1 + k_3 C_B^s + k_4 C_C^s + 2k_9 C_{OH^-}^s) \tag{33}$$

$$\frac{\mathrm{d}N_{BCN}}{\mathrm{d}\tau} = \sigma k_9 \frac{C_A^s i_T}{F k_L} \tag{34}$$

If the yields of BCN are relatively small then the previous solutions for galvanostatic operation (Sections 3.2 and 3.1) can be used as a good approximation to predict the concentration variation of all products. In the event of high BCN yields, which are clearly undesirable, exact solution would be required. The predicted concentrations of BCN produced in the undivided cell process are shown in Figs 3 and 4. Increasing the current density of operation decreases BCN yield as less acrylonitrile is available at the surface for reaction. At a current density of $2000\,\mathrm{A\,m^{-2}}$ typical BCN concentrations are 1 to 1.5 wt %, which are in agreement with experimental data obtained in small scale undivided cell electrolyses [7]. These concentrations are lower than experienced in the divided cell process, mainly due to the lower concentration of acrylonitrile used in the undivided cell.

5. Conclusions

An approximate analysis of cyanoethylation reactions has enabled a reaction model to be developed which describes the formation of the major products and by-products from the electrohydrodimerization of acrylonitrile. Simulations of the adiponitrile process reactor using a reasonable reaction model with one electrochemical step shows the effect of important operating parameters such as current density and flow rate on product distribution. A reduction of electrolyte flow rate, without loss of selectivity, may be possible in operation. Thus the steady-state model of the adiponitrile reactor forms the basis for adoption into dynamic simulation and control studies [8]. An important adjustable parameter, α, represents the fraction of the total current density associated with hydrogen evolution. Further data on this parameter will enable the effects of continuous cathode contamination, i.e. continuously increasing rate of hydrogen evolution, to be 'correlated' as a function of time.

References

[1] A. N. Haines, I. F. McConvey and K. Scott, *Electrochim. Acta* **30** (1985) 291.

[2] Y. Arad, M. Levy, I. R. Miller and D. Vofsi, *J. Electrochem. Soc.* **114** (1967) 899.

[3] A. R. Wright, Soc. of Chem. Ind. Meeting, 'Mathematical Modelling of Electrochemical Processes', London, 3 Feb, 1984.

[4] D. E. Danly and C. R. Campbell, 'Technique of Electroorganic Synthesis', Part III Scale-up and Engineering Aspects (edited by N. L. Weinberg and B. V. Tilak) John Wiley and Sons, New York (1982).

[5] W. V. Childs and H. C. Walters, 'Electro-organic Synthesis Technology', AIChE Symp. Series No. 185, Vol. 75 (1979) p. 19–25.

[6] G. M. Mamoor, 'Mass Transfer Studies in Plate and Frame Electrochemical Reactors', PhD Thesis, University of Newcastle upon Tyne, UK (1983).

[7] A. N. Haines, unpublished work.

[8] J. Henderson, I. F. McConvey and K. Scott, I. Chem. E. Annual Research Meeting, Bradford, 14–15 April 1986. I.Chem.E. Symposium Series No. 98.